

HYPERBRANCHED PEI-PEG/DNA POLYPLEX FORMATION: A MOLECULAR DYNAMICS STUDY

PAUL TROFIN, TITUS ADRIAN BEU

Faculty of Physics, Babeş-Bolyai University, Cluj-Napoca, Romania
Corresponding authors: trofinpaul2@gmail.com; titus.beu@ubbcluj.ro

Received June 16, 2023

Abstract. PEGylated PEIs are intensely studied non-viral vectors for gene delivery, having high transfection efficiencies. Using all-atom molecular dynamics simulations, the interaction of hyperbranched polyethylenimine polyethylene glycol (HPEI-PEG) with DNA was investigated for different number of PEG chains per HPEI core, and, to this end, a new CHARMM Force Field for PEG was developed. The obtained force field parameters are validated by the good agreement of structural measures, such as the radius of gyration, with experimental evidence.

The reported investigations reveal an upper bound for the PEG fraction in the modelled HPEI-PEG polymers. The addition of PEG reduces cytotoxicity, increases solubility, while still ensuring a high efficiency of forming polyplexes with DNA. Useful correlations between the copolymer structure and polyplex properties are observed, along with insights on the dynamics of the formation of hydrogen bonds between the HPEI core and DNA.

Key words: polyethylenimine; polyethylene glycol; non-viral vector; all-atom molecular dynamics.

DOI: <https://doi.org/10.59277/RomJPhys.2023.68.618>

1. INTRODUCTION

Cationic polymers are important for gene delivery, as they can form stable complexes with nucleic acids and facilitate the cellular uptake by ensuring a safe transport of genetic material into cells. One major benefit of polycations used as non-viral gene vectors is that they can be tailored for specific delivery protocols. Their structure and molecular weight can be easily varied to achieve the desired biocompatibility, stability, and transfection efficiency [1].

Branched polyethylenimine (PEI) was shown to have slightly superior efficiency of forming DNA-polyplexes over linear PEI, and this was also confirmed by our recent molecular dynamics (MD) simulations [2]. Hyperbranched PEI (featuring multiple branching points) received significant attention in further attempts to favour the formation of such polyplexes [3]. The net positive charge resulting from the excess of protons in HPEI determines the electrostatic attraction between the protonated PEI monomers and the phosphate groups, which condenses DNA and enables its safe delivery to the cell nucleus. This process can be greatly enhanced by using specifically designed non-viral vectors, with particular protonation fractions [4–6]. The cytotoxicity induced by the charge of the PEI chains can be counteracted

by copolymerization of polyethylene-glycol (PEG), which also helps reducing non-specific interactions with other cellular components. By being neutral and hydrophilic, PEG increases the circulation time of the polyplex in the bloodstream [7], and, as will be shown further on, its behaviour is clearly influenced by the structure of the copolymer (not simply by its molecular weight). Since in many cases cell membranes are negatively charged, the uptake of slightly positive PEI-PEG/DNA polyplexes is favoured [11].

In designing effective genetic delivery protocols, MD simulations offer unparalleled atomic and time resolutions, allowing for otherwise unobtainable insights into the dynamics of the involved biological processes. To elucidate aspects of practical relevance related to the condensation of DNA by HPEI-PEG, such as the effect of PEGylation and copolymer structure on the complexation efficiency, we developed an atomistic (CHARMM) force field (FF) for PEG and used it in conjunction with our previously devised FF for PEI, in extensive simulations of solvated HPEI-PEG/DNA polyplexes.

2. CHARMM FORCE FIELD AND VALIDATION

Force fields provide compact mathematical models for the mechanical interactions occurring within molecular systems. Typically, the potential models in current use (such as the CHARMM model that we employ) comprise bonded and non-bonded interactions. The bonded terms refer to bonds, angles and dihedrals, while the non-bonded terms account for van der Waals interactions, modelled by Lennard-Jones potentials (U_{LJ}), and Coulomb interactions. Essentially, each atom will evolve according to the gradient of the potential energy function:

$$\begin{aligned}
 U = & \sum_{bonds} k_b(b - b_0)^2 + \sum_{angles} k_\theta(\theta - \theta_0)^2 + \\
 & + \sum_{dihedrals} k_\chi[1 + \cos(n\chi + \delta)] + \sum_{non-bonded} \left(U_{LJ} + \frac{q_i q_j}{\epsilon_r r} \right) \quad (1)
 \end{aligned}$$

In simple terms, bonds and angles are modelled by harmonic potentials with k_b and k_θ as force constants, with the respective b_0 , and θ_0 as the equilibrium values where energy is minimized. On the other hand, in the potential energy for dihedrals, n stands for the multiplicity of the periodic potential well, and δ is the phase shift. The partial atomic charges q_i and q_j model the electronic density within an atom and its atom pair respectively.

For the PEG and adjacent PEI monomers, the above parameters were optimized using the Force Field Toolkit [12], a plugin of the visualizer VMD 1.9.3 [13], so as to fit quantum mechanical target data generated using Gaussian [14]. Multiple energy minimization iterations have been performed to ensure convergence of these parameters. For adjacent PEI and PEG, it was imposed that the partial atomic

charges remain unchanged from the already optimized homogeneous polymers. The parameters obtained for a PEG model trimer best reproduced the potential energy functions for a PEG tetramer and a pentamer. Given the additivity of the CHARMM FF model, these parameters can be utilized for arbitrarily long chains.

Table 1

Optimized parameters for the backbone atoms in PEG, as well as for adjacent PEI and PEG monomers. Atoms marked with a star belong to PEI

| Atom | q [a.u.] | Bond | k_b [$\frac{\text{kcal}}{\text{mol}\cdot\text{\AA}^2}$] | b_0 [\AA] | Angle | k_θ [$\frac{\text{kcal}}{\text{mol}\cdot\text{rad}^2}$] | θ_0 [degree] |
|------|---------------|------|--|---------------------------|---------|---|------------------------|
| O | -0.316 | O-C | 351.47 | 1.41 | O-C-C | 65.89 | 107.17 |
| C | -0.022 | C-C | 312.22 | 1.51 | C-O-C | 58.66 | 109.94 |
| | | C-C* | 300.93 | 1.51 | O-C-C* | 70.78 | 107.64 |
| | | | | | C-C*-N* | 70.46 | 109.94 |

Essentially, the dihedral potential energy is a periodic function, therefore scans were performed by varying the dihedral angle χ between -90° and $+90^\circ$ relative to the equilibrium value, with a step of 15° . The multiplicity n is chosen based on local symmetry and the dihedral force constants are refined by adjusting the predicted molecular mechanics (MM) potential surface with respect to the quantum mechanical (QM) target data. It is important to note that, by CHARMM convention, the phase shift δ is fixed to either 0° or 180° . The modelled MM torsional energy landscape for the dihedral angles involving the backbone atoms of interest is shown in Fig. 1, along with the QM target profiles.

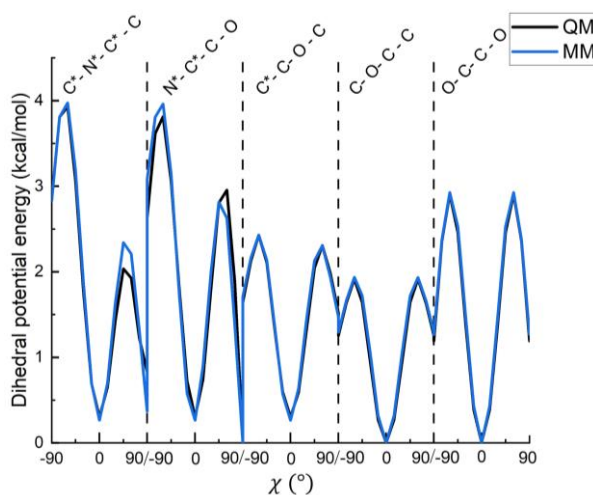


Fig. 1 – Dihedral potential energy for backbone atoms in PEG and adjacent PEI and PEG monomers. Atoms denoted with a star belong to PEI. QM stands for quantum mechanical and MM for molecular mechanical.

For an initial validity test of the obtained parameters, we relaxed a simple $\text{H}_2\text{NC} - \text{PEI} - \text{PEG} - \text{COH}$ structure by simulated annealing using NAMD [16]. After a relaxation of 100 ps, the atomic coordinates changed by only 3.79% on average.

The radius of gyration (R_g) is a measure of how the individual atoms are spread relative to their centre of mass. For single linear PEG chains solvated in water at 300 K, the radius of gyration was calculated as an ensemble average over 10 trajectories of 10 ns, considering only the last 8 ns of each trajectory to ensure proper thermal equilibration of the polymer chains.

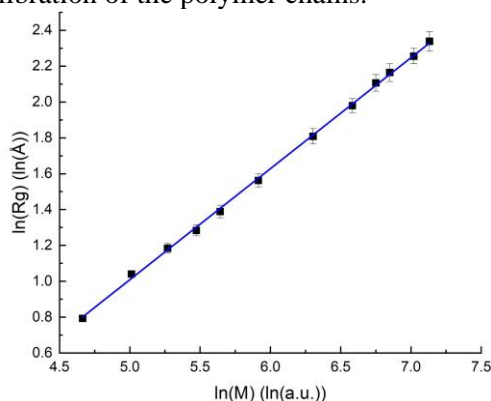


Fig. 2 – The log-log plot of the radius of gyration R_g as a function of the PEG chain mass M .

Figure 2 reveals the power-law dependence of the radius of gyration on the mass (M), with the exponent indicating the slope in the linearized fit:

$$R_g \propto M^{0.619 \pm 0.006} \quad (2)$$

According to the Flory theory of polymers [17], an ideal freely jointed chain is characterized by an 1/2-exponent. The roughly 20% larger value suggests that PEG adopts more extended conformations than an ideal chain. Notably, our adjusted exponent (0.619) is in good agreement with the experimental values of Le Coeur *et al.* [18] (0.588, obtained using small-angle neutron scattering) and Devanand *et al.* [19] (0.583 ± 0.031 , using elastic light scattering).

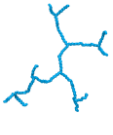
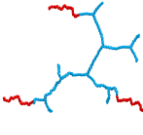
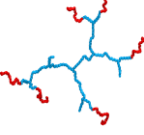
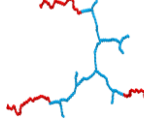

3. SIMULATION METHODS

All the polycations used in our simulations have been constructed based on a HPEI core of 70 monomers with 7 branching points, to which different numbers of PEG chains were attached in different positions. Table 2 summarizes these polycations. Specifically, the notation $\text{PEG}(x)y$ refers to a structure containing y PEG arms with

the length of x monomers. By design, 21 of the 70 PEI monomers composing HPEI have been protonated (bearing a charge of $+1e$) and resulted in a protonation fraction of 0.3 (fraction of protonated groups relative to all amine groups).

Table 2

Copolymer names, composition, molecular weight and structure. HPEI is represented in light blue and PEG in red

| Name | HPEI | HPEI-PEG(10)3 | HPEI-PEG(9)6 | HPEI-PEG(20)3 | HPEI-PEG(18)6 |
|--------------------|---|---|---|--|---|
| PEG content | 0% | 31% | 45% | 47% | 61% |
| Total M_w | 3.4 kDa | 4.5 kDa | 5.7 kDa | 5.9 kDa | 8 kDa |
| Copolymer Geometry |  |  |  |  |  |

The DNA chain was modelled by concatenating three Drew-Dickerson dodecamers (having the A strand $[CGCGAATTCGCG]_3$), a molecular weight of 19.6 kDa, and a total charge of $-62e$ (stemming from the 62 phosphate groups along the backbone). The parameters used for the nucleic acid were taken from CHARMM36 [23], while those for PEI were determined by Beu *et al.* [2, 4–6].

A total of six production trajectories were generated, of which five contain three polycations with DNA, while the last trajectory accommodates four, and is attributed to the best performing copolymer of the five shown in Table 2. No to favor DNA-polycation complexation, the initial configuration was chosen with the copolymers placed perpendicularly to DNA. The systems were solvated with the TIP3P water model and neutralized by adding a single chloride ion.

The largest analysed molecular system consisted of approximately one million atoms, being enclosed in a simulation box with dimensions of $250 \times 380 \times 110$ Å. In the presence of periodic boundary conditions, the z -dimension of the simulation box was chosen so as to exactly accommodate DNA, modelling a virtually infinite chain.

4. SIMULATIONS ANALYSIS AND DISCUSSION

Owing to the electrostatic attraction between the protonated PEI monomers and the negative phosphate groups, the polycations start diffusing towards DNA. After a few nanoseconds, most of the copolymers reach DNA, form the polyplex, and stabilize there for the rest of the simulation.

The analysis of DNA interaction with the cationic copolymers, by evaluating the influence of PEGylation degree on the stability and solubility of the polyplexes, is done sequentially addressing various aspects related to the structure and molecular weight, making a detailed comparison between the utilized gene carriers (summarized in Table 2). Polyplexes not meeting minimal requirements for gene delivery protocols are not considered for full investigation.

Figure 3 outlines the behaviour of DNA interacting with three polycations in the five conducted simulations with increasing PEG content. As can be seen, in the particular case of HPEI-PEG(18)6, only *two* copolymers manage close interaction with DNA. In contrast to the other four cases, the formed polyplex does not achieve a net positive charge, indicating that there is an upper limit for PEGylation degrees still resulting in positive polyplexes. This behaviour evidences the relevance of the geometry and PEG content on DNA complexation, given that DNA overcharging (passing from negative to positive charge) is critical for most gene delivery applications.

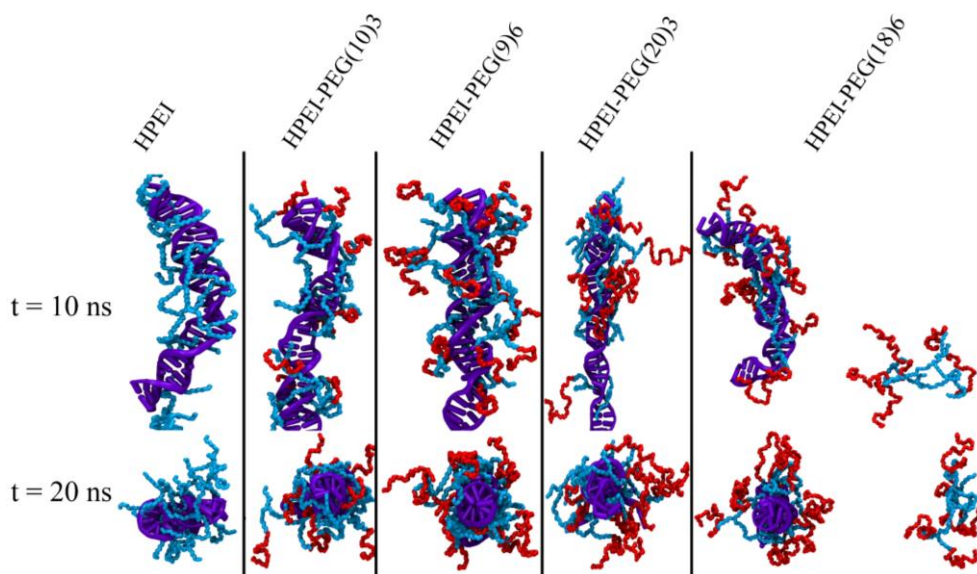


Fig. 3 – Simulation snapshots of the median and last frames (at 10 and 20 ns, respectively) for the five studied DNA-copolymer systems. Color code: DNA (violet), PEI (light blue), and PEG (red).

Upon excluding the system HPEI-PEG(18)6/DNA (right-most panel of Fig. 3), as it forms a negative complex (with reduced cellular uptake efficiency), the binding ability of the four remaining copolymers is characterized by the localization probability density $P_{N^+}(r)$ of protonated nitrogen relative to phosphorus atoms. This is obtained by normalizing the radial pair distribution function, defined as [25]:

$$g(r) = \frac{n(r)}{4\pi r^2 \Delta r \cdot \frac{N_1 N_2}{V}} \quad (3)$$

Essentially, $g(r)$ is the ratio between the average number of atom pairs found at r within a shell of thickness Δr (taken to be 0.1 Å) and the average number of pairs found in the same volume, assuming a homogeneous and isotropic atomic arrangement. In this particular case, N_1 is the number of protonated nitrogens, N_2 the number of phosphorus atoms, and V is the volume of the simulation box. The difference between $g(r)$ and $P(r)$ lies only in the normalization, as we impose that the integral of $P(r)$ converges to 1 for sufficiently large r :

$$P(r) = \frac{g(r)}{\int_0^\infty g(r) dr} \quad (4)$$

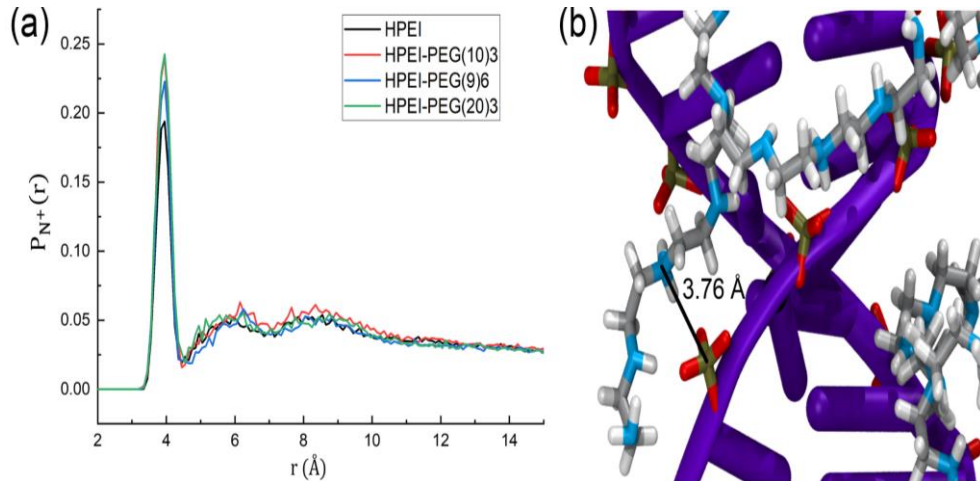


Fig. 4 – Interaction between HPEI and DNA backbone: a) localization probability density $P_{N^+}(r)$ for protonated nitrogen relative to phosphorus atoms; b) close view of HPEI chains around DNA, highlighting the phosphate groups and the distance to a protonated nitrogen. Colour code: carbon (grey), nitrogen (light blue), oxygen (red), phosphorus (ochre), hydrogen (white), and DNA (violet).

All four retained DNA-copolymer systems display a pronounced $P_{N^+}(r)$ -peak around 4 Å, demonstrating the ability of HPEI to condense DNA. Its sharpness suggests the relatively reduced mobility of HPEI around DNA and that hydrogen bonds are formed. Interestingly, the three PEGylated systems show a stronger interaction with the phosphate groups. As indicated by the probability density maxima, the polycations with three PEG arms appear to form complexes slightly more favourably, namely 0.24 for HPEI-PEG(10)3 and HPEI-PEG(20)3, as compared to 0.22 for HPEI-PEG(9)6 and 0.19 for HPEI.

The distribution of PEG chains around DNA is investigated in terms of the localization probability density of PEG-oxygens relative to DNA-phosphorus atoms, denoted $P_0(r)$. In addition, to look into the copolymer-water interaction, the radial distribution function (RDF) $g_w(r)$ of the solvent molecules is calculated relative to the backbone atoms in HPEI and PEG, respectively.

Figure 5a shows significantly broader and less structured probability distributions of PEG around DNA than for HPEI (as shown in Fig. 4a), suggesting an incorporation and shield-like behaviour of PEG around DNA, which can be inferred to reduce the cytotoxicity of the formed polyplexes at a physiological level. In particular, HPEI-PEG(20)3 has the broadest and most right-shifted distribution, which confers DNA increased protection from interacting with other charged biomolecules and cellular components, being likely to result in longer *in vivo* circulation times of the polyplex.

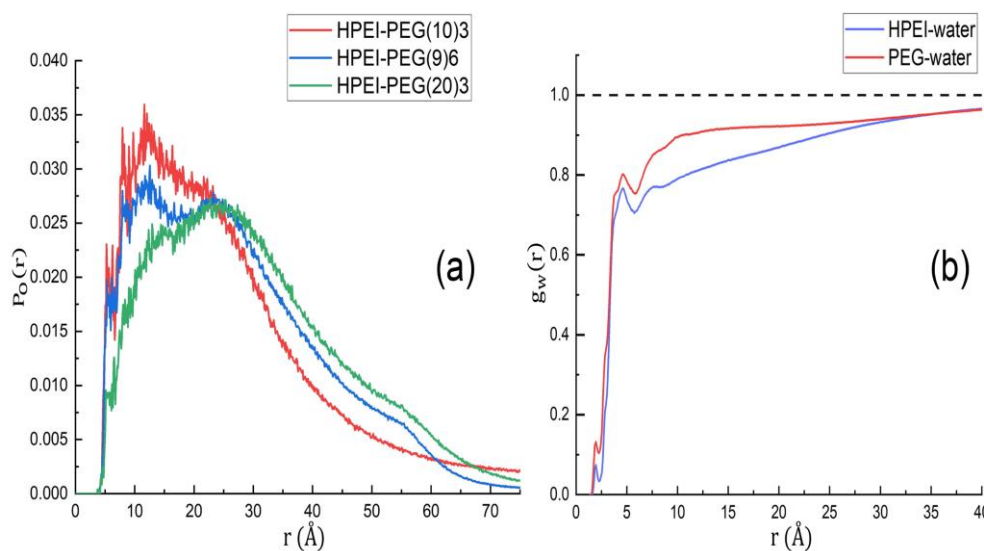


Fig. 5 – PEG distribution and solvent interaction: a) probability density for PEG oxygen atoms with respect to DNA phosphorus atoms; b) radial distribution functions of water around the backbone atoms in HPEI and PEG.

The RDF of the water molecules in Fig. 5b reveals the increased solubility of the PEG chains (averaged over all three PEG-containing systems) in comparison to HPEI (averaged over all four HPEI-containing systems). Each profile presents two local maxima, beyond which they tend asymptotically to 1. The first maximum, around 2 Å, corresponds to the water molecules that are hydrogen bonded to the polymer chains. The second maximum, around 3.5 Å, corresponds to weaker polymer-water interactions and water-water hydrogen bonding. At any particular distance, especially in the range of 5–30 Å, PEG appears to be more hydrophilic

(with more water molecules surrounding it) than HPEI. This correlates well with the PEG probability distributions in Fig. 5a, and it shows that the increased solubility of the polyplex is mainly due to the more extensive conformations of the PEG chains around DNA.

To further analyse the dynamics of DNA complexation with polycations, the time dependence of the hydration shell around the polyplex (DNA and polycations) and the number of hydrogen bonds formed between the HPEI core and DNA was measured. Water molecules have been considered in close proximity of the polyplex for distances below 3 Å. As cut-offs for hydrogen bonding, we have considered 4 Å for the donor-acceptor distances, and 30° for the donor-hydrogen-acceptor angles.

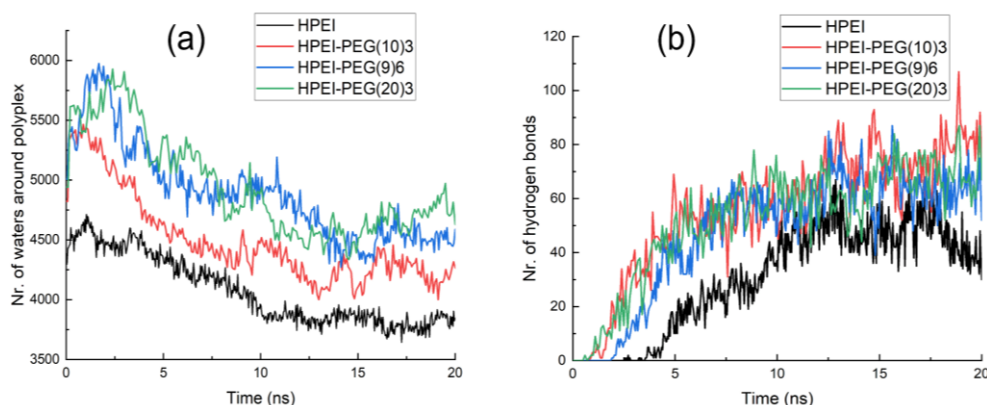


Fig. 6 – Water kinetics and hydrogen bonding: a) number of water molecules around the polyplex; b) number of hydrogen bonds formed between the HPEI core and DNA.

As the polyplexes form, the water molecules are gradually expelled from their vicinity, with the concomitant increase in hydrogen bonds. This explains how hydrogen bonding assists the compounds in reaching stability, which, for our initial system configurations, sets in after about 10 ns.

Mixed HPEI-PEG chains show improved solubility compared to pristine HPEI due to the growth in close-contact water interactions. It is reasonable to conclude that copolymer structures with a higher PEG content exhibit increased solubility. Within statistical fluctuations, the behaviour of water molecules around HPEI-PEG(9)6 and HPEI-PEG(20)3 is similar, suggesting that solubility has a stronger dependence on the PEG molecular weight, than on the polymeric structure. It is interesting to note that the hydration-shell fluctuations are higher for HPEI-PEG than HPEI, because PEG exhibits higher mobility around DNA than HPEI.

Once more, PEGylated HPEIs show a slight increase in stability over HPEI, owing to the more numerous hydrogen bonds. The majority of these bonds are formed between the polar oxygen atoms in the phosphate groups, as acceptors, and

HPEIs backbone atoms, as donors. While finding anew that the Coulomb attraction is the primary drive for polyplex formation, we note that the weaker hydrogen bonds help stabilizing the complexes.

Thus far, the combined ability of HPEI-PEG(20)3 to condense DNA and to form the largest hydrophilic coating, makes it the most promising candidate for gene delivery. To evaluate the saturated DNA complexation, a system composed of four HPEI-PEG(20)3 polycations and the so-far considered DNA chain is analysed. Essentially, the maximum number of cationic copolymers able to have close interaction with DNA is investigated.

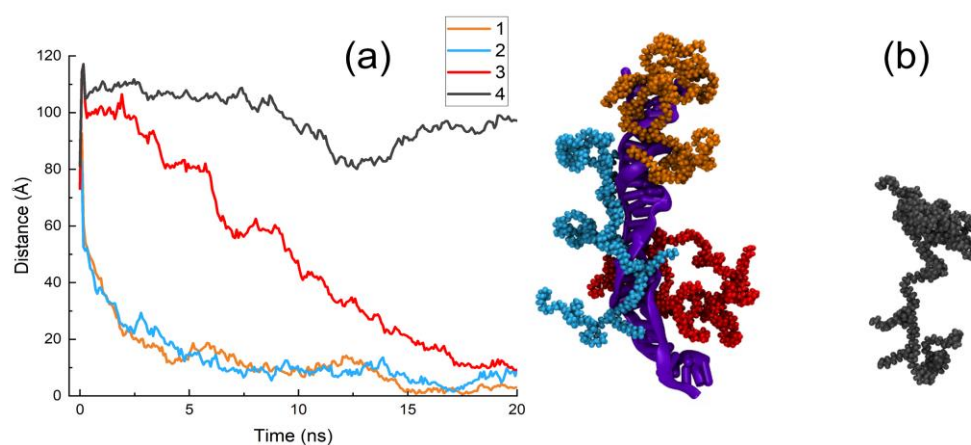


Fig. 7 – Four HPEI-PEG(20)3 interacting with DNA (violet): a) time dependence of polycations centres of mass relative to DNA; b) the last frame of the simulation. The three interacting polycations are 1 (orange), 2 (light blue), 3 (red) and the non-interacting polycation is 4 (dark grey).

For each individual copolymer that engages with DNA, the distance was measured between the centre of mass of the polycation and the phosphate group that showed closest interaction. In the case of the non-interacting copolymer (see Fig. 7b), its distance was measured relative to the DNA's centre of mass. After polycations 1 and 2 reach the DNA chain, the electrostatic potential near the forming polyplex becomes considerably less negative. As a consequence, polycation 3 experiences slower diffusion, and as it approaches DNA, the complex passes the threshold from a negative to a positive net charge, achieving DNA overcharging. Since there is virtually no engagement of polycation 4, complete DNA complexation is reached at $N/P = 3.39$, with N being the number of PEI units, and P the number of DNA-backbone phosphates. This ratio essentially characterizes the set in of the DNA condensation.

In a more general sense, as DNA tends to neutralize, it attracts many cationic copolymers. Once DNA is fully saturated with gene vectors, it no longer interacts with other polycations in the solution.

The results in this work are consistent with experimental evidence from Mao *et al.* [26], which measured an N/P ratio of 3 for PEI structures with numerous branching points, having a PEG ratio of 50%. They also concluded that gene carriers with high degrees of PEGylation and rather short PEG arms are unable to protect nucleic acids against degradation. MD simulations performed by Ziebarth *et al.* [27], in which linear protonated PEI chains were added sequentially near DNA, resulted in a value of 3.5 for the N/P ratio, in very good agreement with our results.

5. CONCLUSIONS

This work aims to demonstrate that the geometry of HPEI-PEG gene carriers has a decisive influence on the properties and behaviour of polyplexes. Structures with a high PEG content and high PEGylation degree are unable to accomplish DNA overcharging, which is paramount for most gene delivery applications. Nevertheless, this implies that PEG content can influence the N/P ratio, which may have to be adjusted according to several factors, including the specific cell type being targeted.

A fundamental role of PEG is to improve solubility, which is seen by both the radial distribution function of water molecules with respect to PEG in comparison to HPEI, and by the increased number of close contact water interactions with the polyplexes. By forming a hydrophilic coating, as shown by the probability distribution of PEG chains around DNA, the polyplexes acquire increased protection against degradation. The association between the PEG chains probability and the RDF of water proves that the increase in solubility is largely due to the swelling contribution of the PEG arms.

The behavioural differences between HPEI and PEG are mainly due to the protonated amine groups, as they display sharply peaked equilibrium distributions relative to phosphorus atoms, causing the water molecules to be ejected from the near vicinity of DNA. Owing to these aspects, weak hydrogen bonds are able to form and help stabilizing the complex.

We were able to confirm that constructing non-viral gene vectors containing PEI-PEG is a sensitive process, as choosing the right length and density of PEG arms influences solubility, stability, and the N/P ratio, which is a critical quantity for the transfection efficiency. Moreover, it is found that polycation structures with fewer, but longer PEG chains per HPEI core, are more stable and provide enhanced protection for the polyplex.

Acknowledgements. One of the authors (PT) gratefully acknowledges a Scientific and Technological Advanced Research scholarship from the Babeş-Bolyai University.

REFERENCES

1. R. Narain, *Polymers and Nanomaterials for Gene Therapy*, Elsevier, Woodhead Publishing, Cambridge UK, 2016.
2. A. E. Terteci-Popescu and T. A. Beu, *Journal of Computational Chemistry* **43**(31), 2072–2083 (2022).
3. J. Wang, H. Wang, P. Zhao, Z. Chen, and Q. Lin, *Colloid and Interface Science Communications* **50**, 100647 (2022).
4. T. A. Beu and A. Farçaş, *Journal of Computational Chemistry* **38**(27), 2335–2348 (2017).
5. T. A. Beu, A. E. Ailenei, and A. Farçaş, *Journal of Computational Chemistry* **39**(31), 2564–2575 (2018).
6. T. A. Beu, A. E. Ailenei, and A. Farçaş, *Chemical Physics Letters* **714**, 94–98 (2019).
7. A. Kichler, *The Journal of Gene Medicine: A cross-disciplinary journal for research on the science of gene transfer and its clinical applications* **6**(S1), S3–S10 (2004).
8. H. Petersen, P. M. Fechner, A. L. Martin, K. Kunath, S. Stolnik, C. J. Roberts, ... and T. Kissel, *Bioconjugate Chemistry* **13**(4), 845–854 (2002).
9. D. Appelhans, H. Komber, M. A. Quadir, S. Richter, S. Schwarz, J. van der Vlist, ... and B. Voit, *Biomacromolecules* **10**(5), 1114–1124 (2009).
10. L. J. R. Foster, *Biopolymers*, 243–256 (2010).
11. U. Lungwitz, M. Breunig, T. Blunk, and A. Göpferich, *European Journal of Pharmaceutics and Biopharmaceutics* **60**(2), 247–266 (2005).
12. C. G. Mayne, M. Muller, and E. Tajkhorshid, University of Illinois at Urbana-Champaign, 2015.
13. W. Humphrey, A. Dalke, and K. Schulten, *J. Molec. Graphics* **14**, 1, 33–38 (1996).
14. Gaussian 09, Revision E.01, Gaussian, Inc., Wallingford CT (2009).
15. R. Dennington, T. A. Keith, and J. M. Millam, GaussView, Version 6.1, Semichem Inc., Shawnee Mission, KS (2016).
16. J. C. Phillips, D. J. Hardy, ... and E. Tajkhorshid, *Journal of Chemical Physics*, 153:044130 (2020).
17. H. Orland, *Journal de Physique I*, 4(1), 101–114 (1994).
18. C. Le Coeur, J. Teixeira, P. Busch, and S. Longeville, *Physical Review E* **81**(6), 061914 (2010).
19. K. Devanand and J. C. Selser, *Macromolecules* **24**(22), 5943–5947 (1991).
20. C. E. Gallops, C. Yu, J. D. Ziebarth and Y. Wang, *Acs Omega* **4**(4), 7255–7264 (2019).
21. I. Kim, T. A. Pascal, S. J. Park, M. Diallo, W. A. Goddard III and Y. Jung, *Macromolecules* **51**(6), 2187–2194 (2018).
22. R. Mészáros, L. Thompson, M. Bos, I. Varga and T. Gilányi, *Langmuir* **19**(3), 609–615 (2003).
23. K. Hart, N. Foloppe, C.M. Baker, E.J. Denning, L. Nilsson, and A.D. Jr. MacKerell, *Journal of Chemical Theory and Computation* **8**, 348–362 (2012).
24. H. Bekker, H. J. C. Berendsen, E. J. Dijkstra, S. Achterop, R. Vondrumen, D. Vanderspoel, ... and M. K. R. Renardus, in 4th International Conference on Computational Physics (PC 92), pp. 252–256, World Scientific Publishing, 1993.
25. B. G. Levine, J. E. Stone, and A. Kohlmeyer, *Journal of Computational Physics* **230**(9), 3556–3569 (2011).
26. S. Mao, M. Neu, O. Germershaus, O. Merkel, J. Sitterberg, U. Bakowsky and T. Kissel, *Bioconjugate Chemistry* **17**(5), 1209–1218 (2006).
27. J. D. Ziebarth, D. R. Kennetz, N. J. Walker and Y. Wang, *The Journal of Physical Chemistry B* **121**(8), 1941–1952 (2017).
28. Z. Wei and E. Luijten, *The Journal of Chemical Physics* **143**(24), 243146 (2015).